# A New Mathematical Model Quantifying Drug Release from Bioerodible Microparticles Using Monte Carlo Simulations

**Juergen Siepmann,[1–3] Nathalie Faisant,[2] and Jean-Pierre Benoit[2]**

*Received May 13, 2002*

***Purpose.*** The major objectives of this study were to 1) develop a new mathematical model describing all phases of drug release from bioerodible microparticles; 2) evaluate the validity of the theory with experimental data; and 3) use the model to elucidate the release mechanisms in poly(lactide-co-glycolide acid)-based microspheres.
***Methods.*** 5-Fluorouracil-loaded microparticles were prepared with an oil-in-water solvent extraction technique and characterized *in vitro*. Monte Carlo simulations and sets of partial differential equations were used to describe the occurring chemical reactions and physical mass transport phenomena during drug release.
***Results.*** The new mathematical model considers drug dissolution, diffusion with nonconstant diffusivities and moving boundary conditions, polymer degradation/erosion, time-dependent system porosities, and the three-dimensional geometry of the devices. In contrast with previous theories, this model is able to describe the observed drug release kinetics accurately over the entire period of time, including 1) initial "burst" effects; 2) subsequent, approximately zero-order drug release phases; and 3) second rapid drug release phases. Important information, such as the evolution of the drug concentration profiles within the microparticles, can be calculated.
***Conclusions.*** A new, mechanistic mathematical model was developed that allows further insight into the release mechanisms in bioerodible microparticles.

**KEY WORDS:** mathematical modeling; bioerodible microparticle; release mechanism; Monte Carlo simulation; erosion.

## INTRODUCTION

The mathematical modeling of drug release from bioerodible delivery systems is not as advanced as the modeling of diffusion- or swelling-controlled devices because the underlying mechanisms are generally more complex (1–3). In addition to physical mass transport phenomena, chemical reactions (e.g., polymer chain cleavage) have to be considered. These reactions continuously alter the conditions for the occurring mass transport processes (4,5). Yet, up to now, no comprehensive mathematical model has been reported in the literature describing accurately all phases of drug release from polymeric bioerodible microparticles, including 1) initial "burst" effects; 2) subsequent, approximately zero-order drug release phases; and 3) second rapid drug release phases.

The major benefits of having found or newly developed adequate mathematical theories for advanced drug delivery systems include the possibility of 1) gaining further insight into the underlying drug release mechanisms and 2) facilitating the optimization of the devices (6). For example, the effect of the composition and geometry (size and shape) of the dosage form on the resulting drug release patterns can be simulated (7).

Upon contact with the release medium, various chemical and physical processes occur in bioerodible drug delivery systems, such as 1) water imbibition into the system (caused by concentration gradients); 2) drug dissolution (if the drug is not molecularly dispersed throughout the system); 3) polymer chain cleavage; 4) diffusion of the drug and of polymer degradation products out of the device (because of concentration gradients); 5) the creation of water-filled pores; and 6) the breakdown of the polymeric structure once the system becomes unstable. Diffusional processes can occur predominantly through the polymer matrix, predominantly through water-filled pores, or through both, the macromolecular network and water-filled cavities in parallel and/or sequence. In certain cases, the polymer degradation products can significantly alter the microenvironmental conditions, e.g., $H^+$ concentration. For example, monomeric and oligomeric acids are generated upon poly(lactide-co-glycolide acid) (PLGA) degradation and can cause significantly decreasing pH values within the dosage forms (8). Because the hydrolytic ester bond chain cleavage is catalyzed by protons, the decreasing micro pH can lead to autocatalytic effects and, thus, accelerated polymer degradation (9,10). However, the imbibition of hydroxide ions from the release medium into the system and/or the diffusion of the generated monomeric/oligomeric acids out of the device can be rapid enough to prevent acidic microenvironments. In these cases, autocatalytic effects are suppressed (11,12). The relative diffusion velocities of the involved acids and bases and, thus, the occurrence/suppression of autocatalytic effects are primarily a function of the size and porosity of the system.

Generally, bi- or triphasic drug-release behavior is observed from bioerodible microparticles (2,13). Despite the continuously growing practical importance of this type of advanced drug delivery system, the underlying release mechanisms are not yet fully understood, and only a few mathematical models have been reported in the literature quantifying drug release from bioerodible microparticles (2). Roughly, these theories can be divided into two categories: 1) empirical models, which usually assume a single, zero-order process controlling the overall drug release rate, and 2) mechanistic models considering specific physicochemical phenomena, such as diffusional mass transport and/or chemical reactions. A subclass of the latter models simulates polymer degradation as a random event using Monte Carlo techniques. In contrast to mechanistic theories, empirical models are not based on the exact description of the involved, real physical, and/or chemical processes. Empirical models only describe the resulting, apparent drug release rates. For example, the superposition of various different phenomena, such as water and drug diffusion, polymer swelling, and polymer degradation, can lead to overall zero-order drug release kinetics. In this case, an empirical model only gives the zero-order equation, whereas mechanistic theories describe the specific underlying chemical and physical processes. Clearly, empirical

[1] College of Pharmacy, Freie Universitaet Berlin, Kelchstr. 31, 12169 Berlin, Germany.
[2] INSERM ERIT-M 0104, College of Pharmacy, Université d'Angers, 10 rue André Boquel, 49100 Angers, France.
[3] To whom correspondence should be addressed. (e-mail: siepmann@zedat.fu-berlin.de)


0724-8741/02/1200-1885/0 © 2002 Plenum Publishing Corporation

models are easier to use, but mechanistic theories are generally more accurate and much more powerful when simulating the effect of device design variables on the resulting drug release patterns (2).

The theories developed by Hopfenberg (14) and Cooney (15) are examples for empirical mathematical models for erodible drug delivery systems, whereas Heller and Baker (16) and Lee (17) presented mathematical approaches that consider specific physicochemical phenomena. Zygourakis (18,19) was the first to use Monte Carlo techniques to simulate polymer degradation in drug delivery systems. This was a major improvement because the time-dependent state of the system could be described more realistically than before. Both, polymer degradation (simulated with Monte Carlo techniques) and diffusional mass transport processes (described using Fick's second law of diffusion) are taken into account in the interesting and comprehensive models developed by Göpferich (20–22). Good agreement with experimental data was achieved, but these theories were developed for cylindrical implants, not for spherical microparticles. Kalampokis *et al.* (23,24) presented a mathematical theory using Monte Carlo simulations to study the process of intestinal drug absorption. A tube model considering the heterogeneous characteristics of the gastrointestinal tract structure was developed. The small intestinal transit flow was simulated using two different diffusion models and a random, dendritic-type internal structure was taken into account. This interesting theory is able to describe the flow, dissolution, and absorption of a drug in the intestine. Bunde *et al.* (25) developed a model quantifying the escape rate of diffusing drug particles from one-, two-, and three-dimensional boxes as well as from percolation fractals. Two cases were studied: the ideal case, where the diffusing particles do not interact with each other, and the more realistic case, where such interactions occur. Charlier *et al.* (26) presented an interesting theory quantifying drug release from thin PLGA films, considering drug diffusion with time-dependent diffusion coefficients (to account for polymer degradation). They obtained good agreement with experimental data, but the model was developed for thin films, not for spherical microparticles.

Recently, we developed a new and simple mathematical model that describes the first two phases of drug release (initial "burst" and subsequent, approximately zero-order kinetics) from PLGA-based microparticles rather well (27,28). However, systematic deviations between theory and experiments were observed, indicating that not all important chemical and physical processes were adequately taken into account (e.g., polymer degradation was not simulated using Monte Carlo techniques). The major advantage of this model is its simplicity, the easiness with which it can be handled. A significant restriction is the lack of considering the final breakdown of the polymeric network once the system becomes unstable upon erosion. Thus, it is not possible to describe triphasic drug release patterns with this theory.

The major objectives of the present study were to 1) develop a new, mechanistic mathematical model that takes into account the most important processes involved in drug release from erodible microparticles (drug dissolution, diffusion with nonconstant diffusivities and moving boundary conditions, polymer erosion based on Monte Carlo simulations, time-dependent system porosities, and the three-dimensional spherical geometry of the devices); 2) evaluate the validity of this model with experimental data, covering all phases of drug release; and 3) use the model to gain further insight into the underlying mass transport phenomena during drug release (e.g., calculation of the time-dependent drug concentration profiles within the system).

## EXPERIMENTAL SECTION

### Materials

PLGA (Resomer® RG 506; PLGA 50:50; containing 25% D-lactic units, 25% L-lactic units and 50% glycolic units, weight-average molecular weight: approximately 104 kDa) and 5-fluorouracil (5-FU) were obtained from Boehringer Ingelheim (Paris, France) and Roche (Neuilly sur Seine, France), respectively.

### Methods

5-FU-loaded PLGA microparticles were prepared with an oil-in-water (O/W) solvent extraction technique. (For details on the preparation and characterization methods, see reference 27.) Briefly, the drug was dispersed and the polymer dissolved within dichloromethane. This organic phase was then emulsified into an aqueous polyvinyl alcohol solution. After adding water and further stirring, the hardened microparticles were separated by filtration, freeze dried, sieved, and vacuum dried. The actual drug loading was determined by dissolving microparticles in dimethylsulfoxide and subsequent UV drug detection. The particle diameter was measured with a Coulter Counter. *In vitro* drug release in phosphate buffer pH 7.4 (37°C) was determined by placing microparticles within dialysis bags at the bottom of USP XXIV paddle apparatus glass vessels. At predetermined time intervals, samples were withdrawn and analyzed UV-spectrophotometrically. Each experiment was conducted in triplicate.

## RESULTS AND DISCUSSION

### *In Vitro* Drug Release Kinetics

The experimentally determined *in vitro* release kinetics from 5-FU-loaded PLGA-based microparticles in phosphate buffer pH 7.4 are illustrated in Fig. 1. Clearly, three different phases can be distinguished: 1) an initial "burst": in which approximately 38% of the drug is released within the first 2 days; 2) a subsequent, approximately zero-order drug release phase from 3 to 16 days (constant relative release rate = 2.6%/day; coefficient of determination, $R^2 = 0.99$); and 3) a second rapid drug release phase, leading to complete drug exhaustion within 3 days. From the shape of the release profile, it is evident that different chemical and/or physical processes are involved in the control of drug release. Clearly, not only one single mechanism (e.g., drug dissolution or diffusion) is dominant throughout the entire period of time. To be able to explain the observed complex drug release behavior, a new mathematical model was developed taking into account different chemical and physical processes simultaneously.

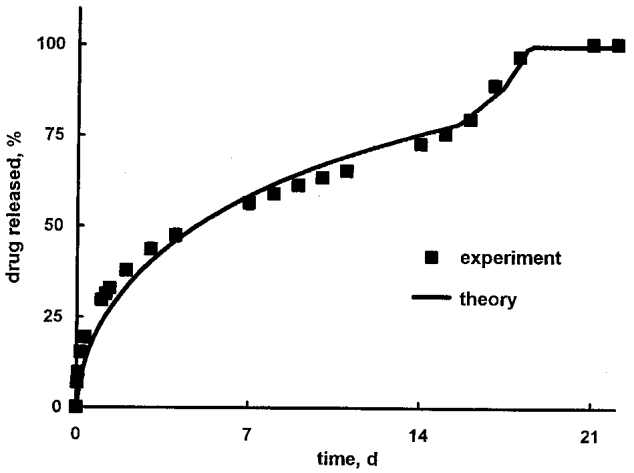


**Fig. 1.** Triphasic drug release kinetics from PLGA-based microparticles in phosphate buffer pH 7.4: experimental data (symbols) and fitted theory (curve) (5-FU, 24% w/w initial drug loading, mean particle diameter = 52 μm).

### Modeling Polymer Degradation/Erosion

Polymer degradation is a random process (2). Upon water imbibition into the PLGA matrix, the polymer backbones start to be cleaved hydrolytically (ester bonds). As the diffusion rate of water into the system is much higher than the degradation rate of the polymer, the entire microparticle is rapidly hydrated and the polymer chains are cleaved throughout the device (bulk erosion). Because of the complexity of the system, it is not possible to predict the exact time point at which a particular ester bond located at a specific position within the macromolecular network is cleaved. Instead, Monte Carlo techniques can be used to simulate the random degradation behavior of a large population of cleavable polymer bonds with sufficient accuracy (21,22). In the following, the principle of such a technique applied to calculate the time-dependent composition of the multi-component system "polymer-drug-water" is described.

Figure 2a shows a schematic presentation of a spherical microparticle for mathematical analysis. To minimize computation time, the origin of the coordinate system is placed at the center of the sphere. It is assumed that the microparticle is rotational symmetric to the angle θ. Thus, a two-dimensional grid (Fig. 2b) can be defined, which upon rotation around the z-axis describes the three-dimensional structure of the sphere. Each pixel in the two-dimensional grid represents either polymer or drug (before the system is exposed to the release medium). All pixels have the same height but different widths. The coordinates are chosen in such a way that the volumes of the cylindrical rings, which are described by the rectangular pixels upon rotation around the z-axis, are all equal. This assures equal numbers of cleavable ester bonds within each ring. Thus, the probability with which the polymer pixels erode within a certain time period after contact with water can be assumed to be very similar (being essentially a function of the number of cleavable polymer bonds). Because polymer degradation is a random process, not all pixels degrade exactly at the same time point. They possess individual, randomly distributed "lifetimes." For reasons of simplicity, polymer degradation and the subsequent diffusion of the degradation products out of the device are simulated as

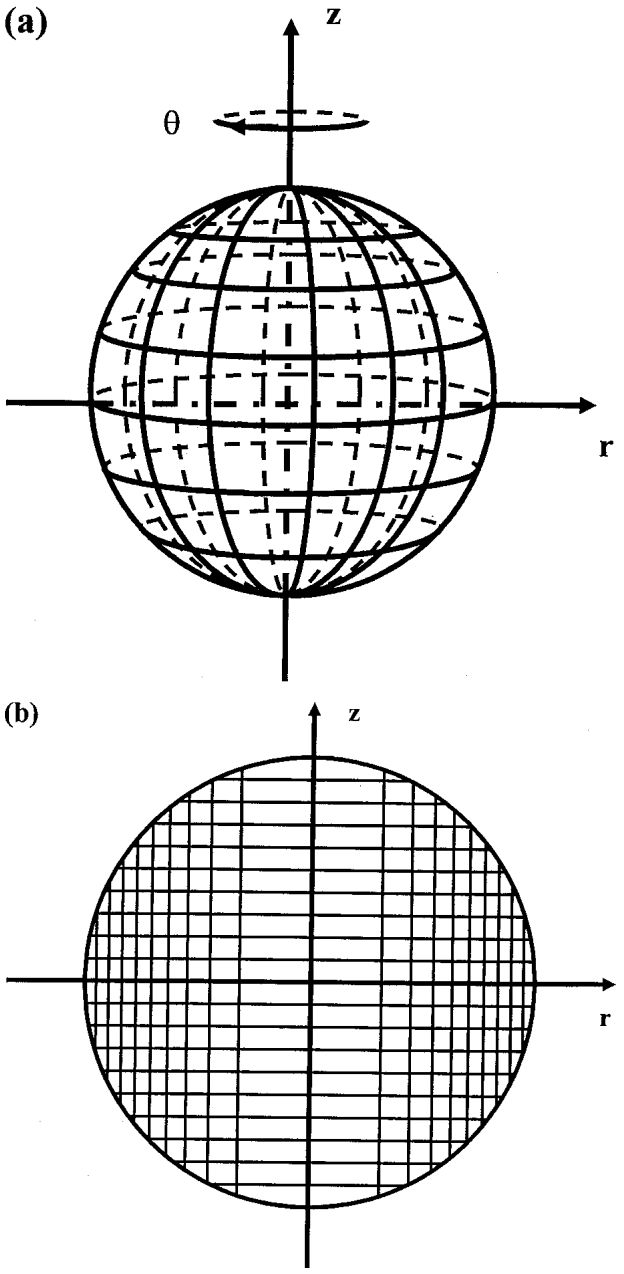


**Fig. 2.** Schematic of a single bioerodible microparticle for mathematical analysis: (a) three-dimensional geometry; (b) two-dimensional cross-section with two-dimensional pixel grid used for numerical analysis.

one event (polymer erosion). As soon as a pixel comes into contact with water, its "lifetime" starts to decrease. After the latter has expired, the pixel is assumed to erode instantaneously. The "lifetime," $t_{\text{lifetime}}$, of a pixel is calculated as a function of the random variable $\varepsilon$ (integer between 0 and 99):

$$t_{\text{lifetime}} = t_{\text{average}} + \frac{(-1)^{\varepsilon}}{\lambda} \cdot \ln\left(1 - \frac{\varepsilon}{100}\right) \quad (1)$$

where $t_{\text{average}}$ is the average "lifetime" of the pixels and λ is a constant (being characteristic for the type and physical state of the polymer). Göpferich (21,22) used a similar equation to calculate the individual "lifetimes" of polymer pixels in bio-

erodible implants, picking them at random from a first-order Erlang distribution. The idea is to treat the erosion of a polymer pixel as a random event, which can be described by a Poisson process of first order. As amorphous polymer pixels erode faster than crystalline ones, it is important to take the physical state of the polymer adequately into account when calculating the "lifetimes" of the pixels upon contact with water.

### Modeling Drug Dissolution and Diffusional Processes

Diffusional mass transport processes are described using Fick's second law. As can be seen in Fig. 3a, two symmetry planes exist in the spherical microparticles for the drug, polymer, and water concentration profiles (r = 0 and z = 0, respectively), so that the mathematical analysis can be reduced to one quarter of the sphere. Thus, based on the rotational symmetry around the z-axis (Fig. 2a), the two-dimensional pixel grid shown in Fig. 2b can be reduced to one quarter of the circle (Fig. 3b). As indicated and explained above, this quarter is divided into rectangular pixels, which upon rotation around the z-axis describe cylindrical rings (for most calculations I = J = 100 was chosen). To describe drug diffusion within these rings, Fick's second law for cylindrical devices taking into account axial and radial mass transfer is used (29):

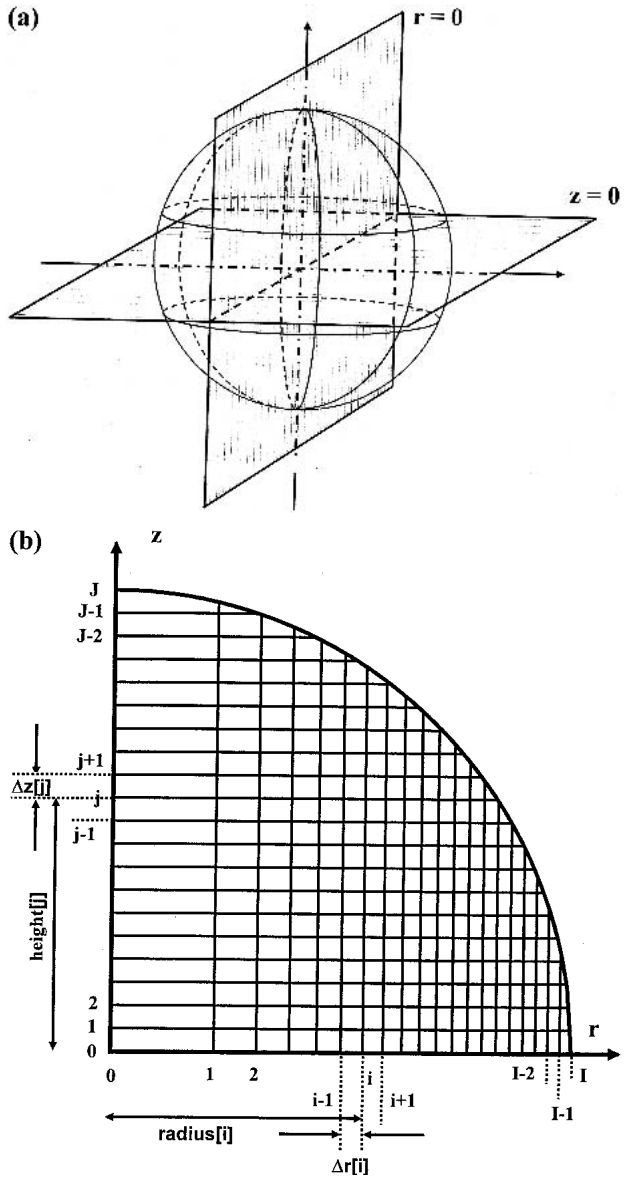


**Fig. 3.** Schematic of a single bioerodible microparticle for mathematical analysis: (a) three-dimensional geometry with two symmetry planes; (b) reduced two-dimensional pixel grid used for numerical analysis.

$$\frac{\partial c}{\partial t} = \frac{1}{r}\left\{\frac{\partial}{\partial r}\left(rD\frac{\partial c}{\partial r}\right) + \frac{\partial}{\partial \theta}\left(\frac{D}{r}\frac{\partial c}{\partial \theta}\right) + \frac{\partial}{\partial z}\left(rD\frac{\partial c}{\partial z}\right)\right\} \quad (2)$$

Here, $c$ and $D$ are the concentration and diffusion coefficient of the drug; $r$ denotes the radial coordinate, $z$ the axial coordinate, $\theta$ the angle perpendicular to both axes (Fig. 2a), and $t$ represents time.

Because there is no concentration gradient with respect to $\theta$, this equation can be transformed into:

$$\frac{\partial c}{\partial t} = \frac{\partial}{\partial r}\left(D\frac{\partial c}{\partial r}\right) + \frac{D}{r}\frac{\partial c}{\partial r} + \frac{\partial}{\partial z}\left(D\frac{\partial c}{\partial z}\right) \quad (3)$$

Ideal mixing is assumed (no volume contraction upon mixing drug, polymer, and water), and the total volume of the system at any instant is given by the sum of the volumes of the single components. The initial conditions reflect the fact that the microparticle is dry and the drug randomly distributed at $t = 0$, as can be seen in Fig. 4a. A direct Monte Carlo technique and the knowledge of the experimentally determined drug loading of the microparticles before exposure to the release medium (24% w/w) are used to calculate the initial drug and polymer distribution patterns. Clearly, no symmetry planes can be considered in this quarter of the two-dimensional circle. One major advantage of the presented mathematical model is that it takes this heterogeneity of the inner structure of the microparticles into account. Upon exposure to the release medium, water rapidly imbibes into the system and dissolves the drug, which subsequently diffuses out of the device. Importantly, the model takes the effect of limited drug solubilities into account. In the case of poorly water-soluble drugs or high initial loadings of moderately water-soluble drugs, dissolved and nondissolved drug coexist within the system. At each time step, the actual concentrations of drug and water are calculated at each grid point within the system. If the total amount of drug exceeds the amount soluble under the actual conditions, the excess is considered to be nondissolved and, thus, not available for diffusion.

The boundary conditions are based on the assumption of perfect sink conditions and on the two symmetry planes shown in Fig. 3a, respectively:

$$t > 0 \quad c = 0 \qquad \sqrt{r^2 + z^2} = R_t \quad (4)$$

$$t > 0 \quad \frac{\partial c}{\partial z} = 0 \qquad 0 \le r \le R_t \quad z = 0 \quad (5)$$

$$t > 0 \quad \frac{\partial c}{\partial r} = 0 \qquad 0 \le z \le R_t \quad r = 0 \quad (6)$$

where $R_t$ is the time-dependent radius of the microparticles (the initial radius before exposure to the release medium, $R_0$, was determined to be equal to 26 μm).

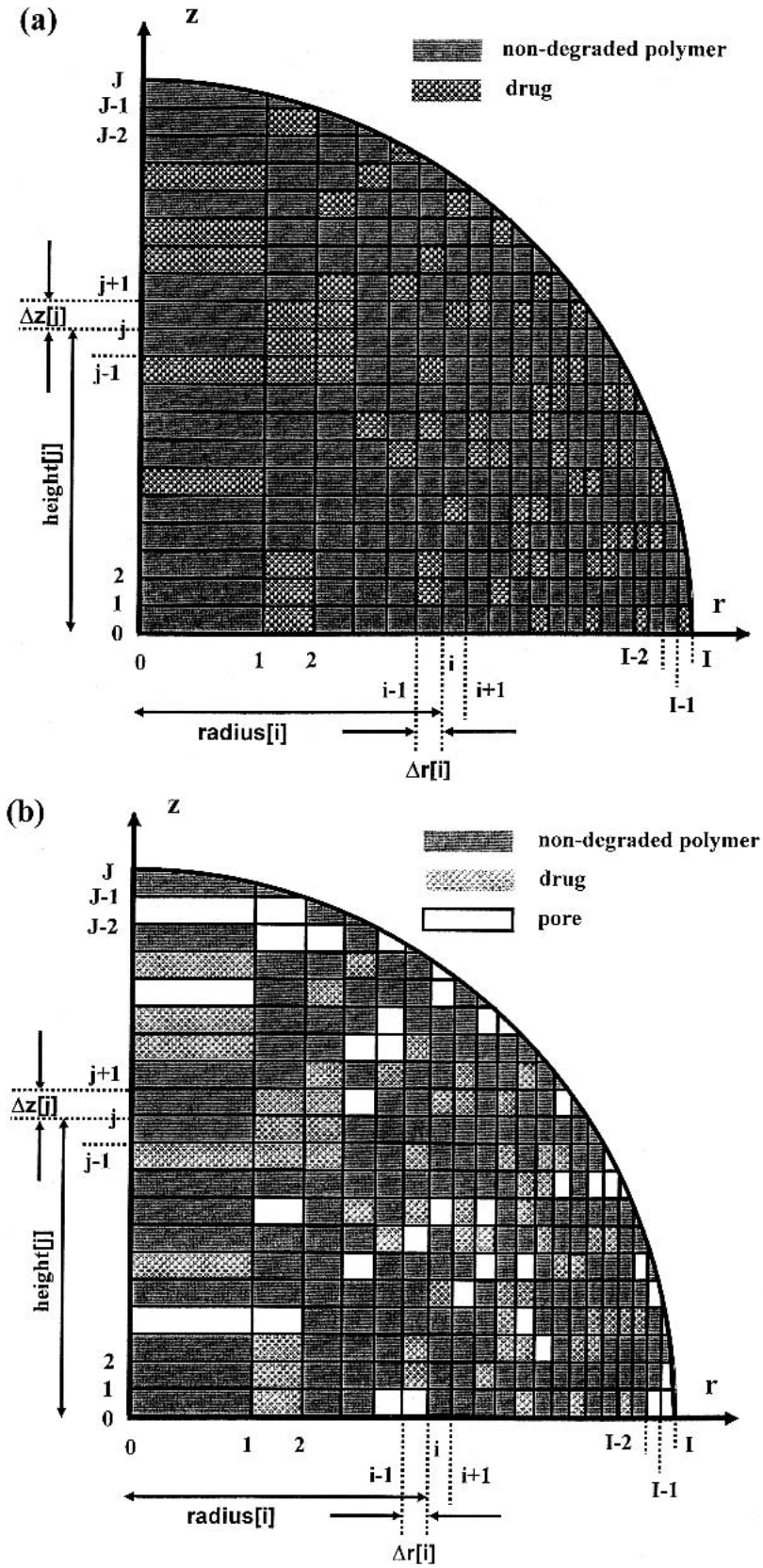


**Fig. 4.** Principle of the Monte Carlo-based approach to simulate polymer degradation and diffusional drug release; schematic structure of the system: (a) at time $t = 0$ (before exposure to the release medium); and (b) during drug release. Gray, dotted, and white pixels represent nondegraded polymer, drug, and pores, respectively.

Because of polymer erosion, the porosity of the matrix increases with time (Fig. 4b). To take this fact adequately into account, a function "*s*" describing the status of the pixel $x_{i,j}$ at time *t* is defined as follows:

$$s(i,j,t) = 1 \quad \text{for non-eroded polymer} \tag{7}$$

$$s(i,j,t) = 0 \quad \text{for pores} \tag{8}$$

Knowing the status of each pixel at each time step from the Monte Carlo simulations, the porosities in radial and axial direction, $\varepsilon(z,t)$ and $\varepsilon(r,t)$, depending on position and time can be calculated as follows:

$$\varepsilon(r,t) = 1 - \frac{1}{n_z} \cdot \sum_{j=1}^{j=n_z} s(i(r),j,t) \tag{9}$$

$$\varepsilon(z,t) = 1 - \frac{1}{n_r} \cdot \sum_{i=1}^{i=n_r} s(i,j(z),t) \tag{10}$$

where $n_z$ and $n_r$ represent the number of pixels in the axial and radial direction at *r* and *z*, respectively. It is important to consider the dependence of the porosity on the direction (axial/radial) because the inner structure of the microparticle is heterogeneous (Fig. 5). Thus, the porosity in radial direction can significantly differ from the porosity in axial direction at the same position. Based on Eqs. (9) and (10), the time- and direction-dependent porosities within the microparticles can be calculated at any grid point. These are essential information for the accurate calculation of the time-, position-, and direction-dependent diffusivities. Based on the porosity values, the diffusivities of the drug, D, in axial and radial direction are calculated as follows:

$$D(r,t) = D_{crit} \cdot \varepsilon(r,t) \tag{11}$$

$$D(z,t) = D_{crit} \cdot \varepsilon(z,t) \tag{12}$$

where $D_{crit}$ represents a critical diffusion coefficient, being characteristic for a specific drug-polymer combination.

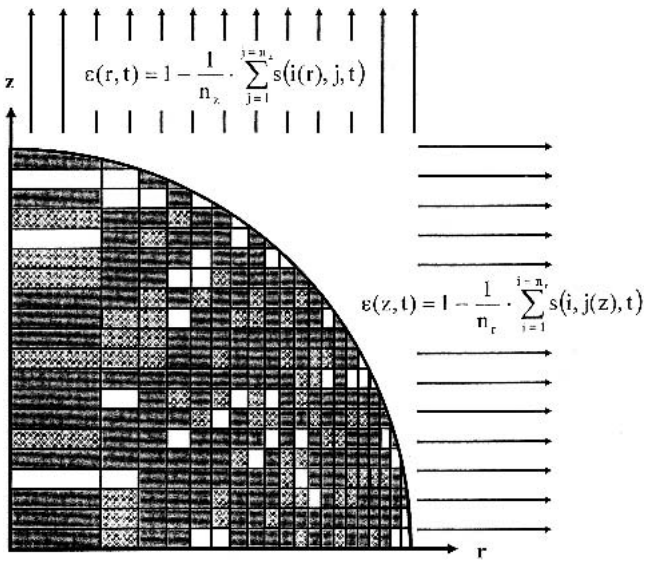


**Fig. 5.** Principle of the calculation of the time and position-dependent radial and axial microparticle porosities, $\varepsilon(z,t)$ and $\varepsilon(r,t)$, during drug release. Gray, dotted, and white pixels represent nondegraded polymer, drug, and pores, respectively.

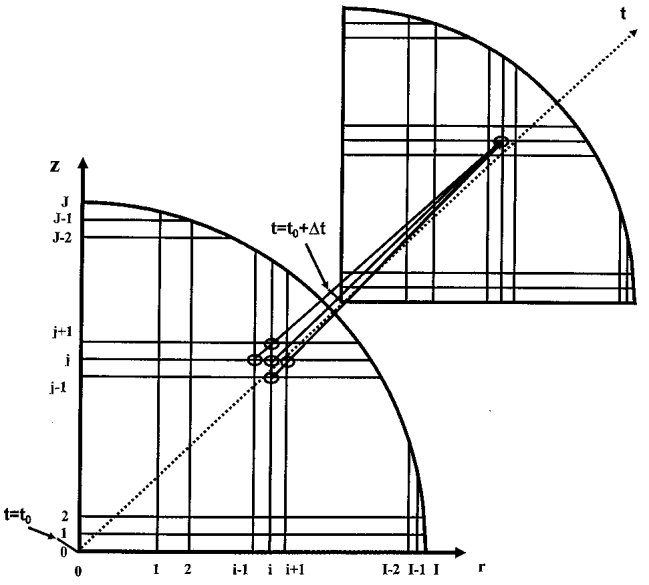


**Fig. 6.** Principle of the numerical analysis: calculation of the concentration profile of the diffusing species at a new time step from the concentration profile at the previous time step.

Owing to the time-dependent composition of the system and the time-, direction- and position-dependent diffusion coefficients, the described set of partial differential equations is solved numerically, using finite differences. The principle of this method is illustrated in Fig. 6. The radius of a microparticle is divided into I-space intervals in radial direction and into J-space intervals in axial direction. The time is divided into g time intervals $\Delta t$ (for most of the simulations g = 500,000 was chosen). Using Eqs. (3) to (12), the concentration profiles for a new time step ($t = t_0 + \Delta t$) can be calculated, when the concentration profiles are known at the previous time step ($t = t_0$). The concentration at a certain inner grid point [*i*][*j*] for the new time step ($t = t_0 + \Delta t$) is calculated from the concentrations at the same grid point [*i*][*j*] and its four direct neighbors [*i* − 1][*j*]; [*i*][*j* − 1]; [*i*][*j* + 1]; [*i* + 1][*j*] at

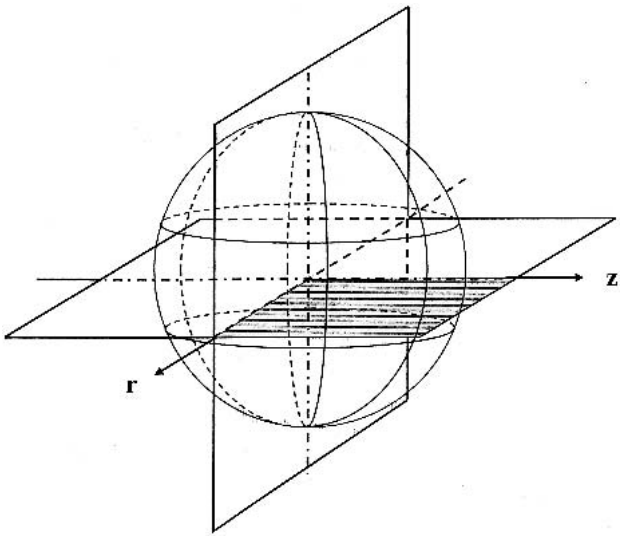


**Fig. 7.** Schematic of a three-dimensional, single microparticle: illustration of the point of view for the calculated drug concentration profiles in Fig. 8.

the previous time step ($t = t_0$) (Fig. 6). The concentrations at the outer grid points (radius[$i$]$^2$ + height[$j$]$^2$ = radius[$I$]$^2$ $v$ $i$ = 0 $v$ $j$ = 0) for the new time step ($t = t_0 + \Delta t$) are calculated using the boundary conditions (Eqs. 4–6). At time $t = 0$, the distribution of the drug within the polymer matrix is simulated using a direct Monte Carlo technique, based on the experimentally determined initial drug loading (24% w/w) (Fig. 4a). Hence, the concentration profiles at $t = 0 + \Delta t$, $t = 0 + 2\Delta t$, $t = 0 + 3\Delta t$,. . ., $t = 0 + g\Delta t$ can be calculated sequentially. The effect of limited drug solubility is taken into account based on the actual concentrations of drug and water at each grid point within the microparticle at each time step. Only the amount of drug that is soluble under the present conditions is considered to be available for diffusion. For the implementation of the mathematical model the programming language C++ was used (Borland C++ 5.02).

### Experiment and Theory

Figure 1 shows the fit of the new mathematical model to the experimentally determined *in vitro* drug release rate from 5-FU-loaded PLGA-based microparticles in phosphate buffer pH 7.4. The fitting procedure was based on the minimization of the resulting differences between experimental and theoretical values (least squares method, combined with a modified simplex method: Nelder-Mead-method). As can be seen, good agreement between theory and experiment was obtained (coefficient of determination, $R^2 = 0.99$). Importantly, all three drug release phases were accurately described.

### Release Mechanism

As can be seen in Fig. 1, the initial "burst" phase is rather well described with the new mathematical model. As polymer degradation is negligible at these early time points (within the first 2 days of drug release), drug dissolution and diffusion are the dominating mass transfer processes. Diffusion-controlled delivery systems generally show high initial drug release rates because of the small diffusion pathways (1). In the present case, the 5-FU diffusion coefficient in the system (being characteristic for a specific drug-polymer combination) was determined to be equal to $6.7 \times 10^{-12}$ cm$^2$/s after 2 days exposure to the release medium, which is a typical value for a drug molecule of that size in a polymeric network (1). However, it has to be pointed out that in specific cases the underlying mechanisms can be more complex. For example, Wang *et al.* (30) showed that pores in the size range of 0.1 to 1 μm were initially ($t = 0$) present at the surface of their system (octreotide acetate-loaded PLGA microparticles), leading to high drug diffusion coefficients. Upon water imbibition and polymer swelling, these surface pores were rather rapidly closed (within 24 h), changing the conditions for drug diffusion drastically.

The intermediate, approximately zero-order drug release phase results from the superposition of at least three phenomena: drug dissolution, diffusion, and polymer erosion. The release rate from purely diffusion-controlled drug delivery systems decreases with time because of the increasing diffusion pathways (surface near regions become depleted) (29). In the present case, the physicochemical characteristics of the system through which the drug diffuses significantly change with time. Upon contact with water, the polymer bonds start to be cleaved, the "lifetimes" of the polymer pixels expire, and pores are created, leading to increased drug diffusion coefficients (from $6.7 \times 10^{-12}$ cm$^2$/s on day 2 to $1.7 \times 10^{-11}$ cm$^2$/s on day 16). This increase in the mobility of the drug molecules partially compensates the increasing diffusion pathways. In addition to the effect of polymer erosion, the limited solubility of the drug can significantly contribute to the overall control of the release rate in systems in which the initial drug loading exceeds the drug solubility. Only dissolved drug molecules can diffuse out of the device; drug molecules in undissolved crystals and amorphous particles are not available for diffusion. To clarify the importance of drug dissolution in the present system, the new mathematical model was used to calculate the time-dependent concentration profiles of the drug within the microparticles upon exposure to the release medium. For reasons of clarity, the concentration gradients within only one quarter of the spheres (Fig. 3b) are presented after 1, 7, and 17 days, respectively. Figure 7 shows the schematic of a three-dimensional, single microparticle and the point of view for the drug concentration profiles which are illustrated in Fig. 8. Figure 8(a, c, and e) shows the complete concentration range, whereas Fig. 8(b, d, and f) shows only the lower concentration range (0 to 30 mg/mL). Clearly, a large excess of drug is present in the system (the solubility of the drug being equal to 19.5 mg/mL). This strongly affects the resulting drug concentration profiles: a pseudo steady state with linear concentration gradients (the driving forces for diffusion) is provided. Because of the high excess of drug, the rate at which the "diffusion front" (separating the zone containing dissolved and undissolved drug from the zone containing only dissolved drug) moves toward the center of the microparticles is rather low. Thus, the diffusion pathways increase only slowly with time and can more easily be compensated by the increasing apparent drug diffusivities, compared to a system in which the drug is completely dissolved at $t = 0$.

A dramatic change of the conditions for the mass transport processes occurs when the polymeric structure of the system becomes unstable and the macromolecular network breaks down. The observed second rapid drug release phase leading to complete drug exhaust within only 3 days can be attributed to this phenomenon: the average "lifetime" of the polymer pixels upon contact with water was found to be equal to 15.6 days. This agrees very well with the onset of the second "burst" (Fig. 1). Because of the significantly increasing drug diffusivities (Eqs. 11 and 12) and the decreasing diffusion pathways, the resulting drug release rate markedly increases.

A second "burst" phase can only occur if drug is still present within the system when the polymeric structure breaks down. If the initial "burst" is more important and/or the subsequent, approximately zero-order drug release is faster and/or lasting longer periods of time drug release is complete before the microparticles loose their integrity. The resulting release patterns are then only biphasic or even monophasic. Importantly, the newly developed mathematical model is also applicable to these cases.

## CONCLUSIONS

A new mathematical model has been developed quantifying drug release from bioerodible microparticles considering drug dissolution, diffusion with nonconstant diffusivities

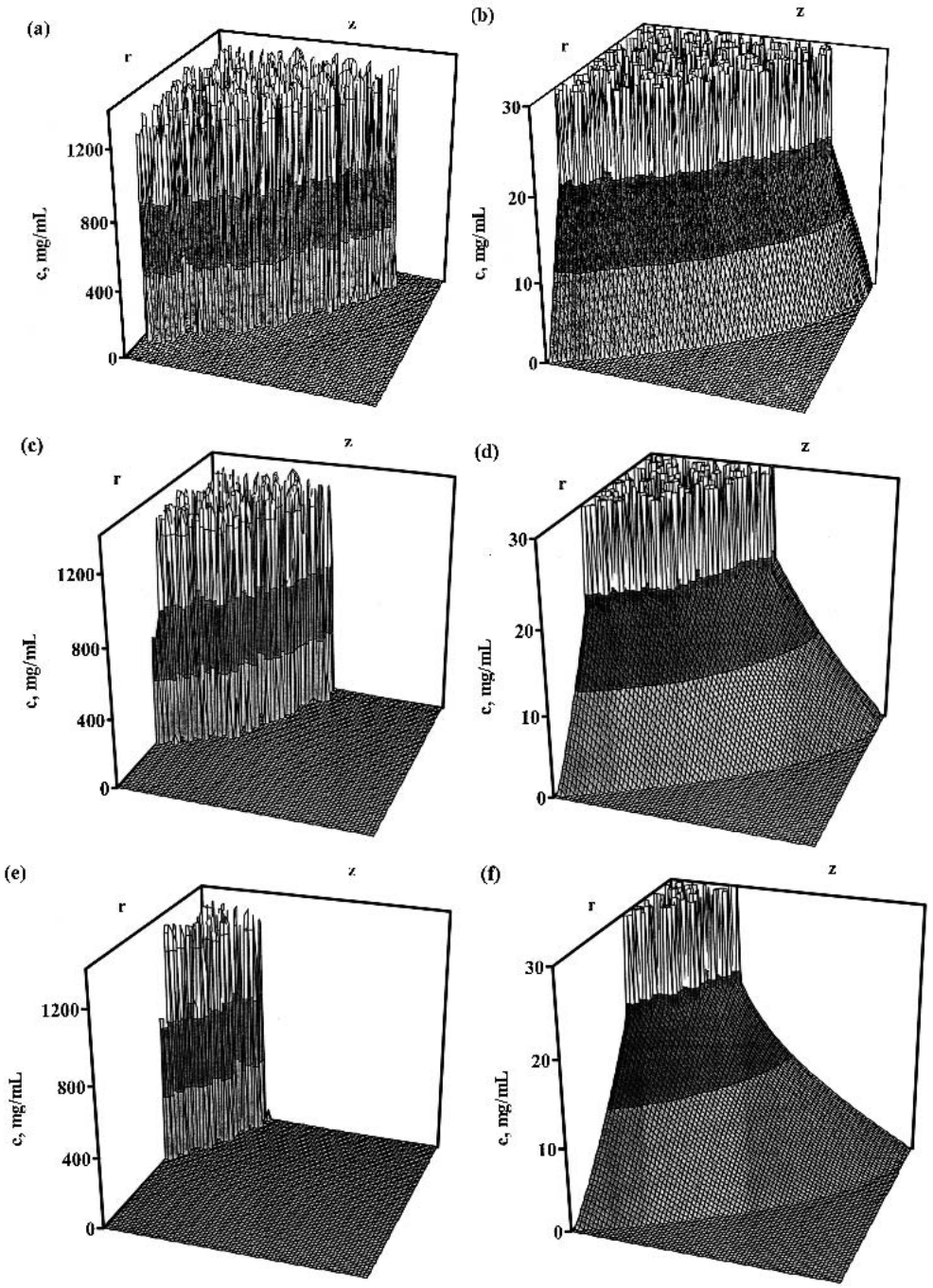


**Fig. 8.** Calculated evolution of the drug concentration profiles within PLGA-based microparticles upon exposure to the release medium: (a) after 1 day, complete concentration range; (b) after 1 day, zoom on low drug concentrations; (c) after 7 days, complete concentration range; (d) after 7 days, zoom on low drug concentrations; (e) after 17 day, complete concentration range; (f) after 17 days, zoom on low drug concentrations (the relative point of view is illustrated in Fig. 7).

and moving boundary conditions, polymer degradation/erosion (based on Monte Carlo simulations), time-dependent system porosities, and the three-dimensional geometry of the devices. In contrast with previous theories, this model accurately describes all three phases of drug release that can be observed: initial "bursts," subsequent approximately zero-order drug release, and second "burst" phases. Importantly, the model allows gaining further insight into the underlying chemical and physical mechanisms involved in the control of drug release. For example, the time-dependent drug concentration profiles and composition of the system can be calculated. An interesting possible practical application of the new model is the prediction of the effect of different formulation and processing parameters on the resulting drug release kinetics from bioerodible microparticles. In future studies the novel theory will be used to quantify the effect of the microparticle size, experimental *in vitro* release conditions and $\gamma$ irradiation on the resulting drug release patterns.

## ACKNOWLEDGMENTS

This work was supported by the European Commission (Marie Curie Individual Fellowship, Contract No. HPMF-CT-

1999-00033; Research and Technological Development Project BCDDS, Contract No. QLK3-CT-2001-02226).

## REFERENCES


1. L. T. Fan and S. K. Singh. *Controlled Release: A Quantitative Treatment*, Springer-Verlag, Berlin, 1989.
2. J. Siepmann and A. Göpferich. Mathematical modeling of bioerodible, polymeric drug delivery systems. *Adv. Drug Deliv. Rev.* **48**:229–247 (2001).
3. J. Siepmann and N. A. Peppas. Modeling of drug release from delivery systems based on hydroxypropyl methylcellulose (HPMC). *Adv. Drug Deliv. Rev.* **48**:139–157 (2001).
4. M. Vert, J. Feijen, A. Albertsson, G. Scott, and E. Chiellini. *Biodegradable Polymers and Plastics*, Redwood Press, Melksham, 1992.
5. A. Göpferich. Polymer degradation and erosion: mechanisms and applications. *Eur. J. Pharm. Biopharm.* **42**:1–11 (1996).
6. J. Siepmann, A. Streubel, and N. A. Peppas. Understanding and predicting drug delivery from hydrophilic matrix tablets using the "sequential layer" model. *Pharm. Res.* **19**:306–314 (2002).
7. J. Siepmann, H. Kranz, N. A. Peppas, and R. Bodmeier. Calculation of the required size and shape of hydroxypropyl methylcellulose matrices to achieve desired drug release profiles. *Int. J. Pharm.* **201**:151–164 (2000).
8. A. Shenderova, T. G. Burke, and S. P. Schwendeman. The acidic microclimate in poly(lactide-co-glycolide) microspheres stabilizes camptothecins. *Pharm. Res.* **16**:241–248 (1999).
9. G. Spenlehauer, M. Vert, J. P. Benoit, and A. Boddaert. In vitro and in vivo degradation of poly(D,L lactide/glycolide) type microspheres made by solvent evaporation method. *Biomaterials* **10**:557–563 (1989).
10. M. Dunne, O. I. Corrigan, and Z. Ramtoola. Influence of particle size and dissolution conditions on the degradation properties of polylactide-co-glycolide particles. *Biomaterials* **21**:1659–1668 (2000).
11. J. M. Anderson and M. S. Shive. Biodegradation and biocompatibility of PLA and PLGA microspheres. *Adv. Drug Del. Rev.* **28**:5–24 (1997).
12. P. Sansdrap and A. J. Moes. In vitro evaluation of the hydrolytic degradation of dispersed and aggregated poly(DL-lactide-co-glycolide) microspheres. *J. Control. Release* **43**:47–58 (1997).
13. H. B. Ravivarapu, K. Burton, and P. P. DeLuca. Polymer and microsphere blending to alter the release of a peptide from PLGA microspheres. *Eur. J. Pharm. Biopharm.* **50**:263–270 (2000).
14. H. B. Hopfenberg. Controlled release from erodible slabs, cylinders, and spheres. In D. R. Paul and F. W. Harris (eds.), *Controlled Release Polymeric Formulations, ACS Symp. Ser. No. 33*, American Chemical Society, Washington, 1976 pp. 26–32.
15. D. O. Cooney. Effect of geometry on the dissolution of pharmaceutical tablets and other solids: Surface detachment kinetics controlling. *AIChE J.* **18**:446–449 (1972).
16. J. Heller and R. W. Baker. Theory and practice of controlled drug delivery from bioerodible polymers. In R. W. Baker (ed.), *Controlled Release of Bioactive Materials*, Academic Press, New York, 1980 pp. 1–18.
17. P. I. Lee. Diffusional release of a solute from a polymeric matrix–approximate analytical solutions. *J. Membr. Sci.* **7**:255–275 (1980).
18. K. Zygourakis. Discrete simulations and bioerodible controlled release systems. *Polym. Prep. ACS* **30**:456–457 (1989).
19. K. Zygourakis. Development and temporal evolution of erosion fronts in bioerodible controlled release devices. *Chem. Eng. Sci.* **45**:2359–2366 (1990).
20. A. Göpferich. Mechanisms of polymer degradation and erosion. *Biomaterials* **17**:103–114 (1996).
21. A. Göpferich. Bioerodible implants with programmable drug release. *J. Control. Release* **44**:271–281 (1997).
22. A. Göpferich. Erosion of composite polymer matrices. *Biomaterials* **18**:397–403 (1997).
23. A. Kalampokis, P. Argyrakis, and P. Macheras. Heterogeneous tube model for the study of small intestinal transit flow. *Pharm. Res.* **16**:87–91 (1999).
24. A. Kalampokis, P. Argyrakis, and P. Macheras. A heterogeneous tube model of intestinal drug absorption based on probabilistic concepts. *Pharm. Res.* **16**:1764–1769 (1999).
25. A. Bunde, S. Havlin, R. Nossal, H. E. Stanley, and G. H. Weiss. On controlled diffusion-limited drug release from a leaky matrix. *J. Chem. Phys.* **83**:5909–5913 (1985).
26. A. Charlier, B. Leclerc, and G. Couarraze. Release of mifepristone from biodegradable matrices: Experimental and theoretical evaluations. *Int. J. Pharm.* **200**:115–120 (2000).
27. N. Faisant, J. Siepmann, and J. P. Benoit. PLGA-based microparticles: Elucidation of mechanisms and a new, simple mathematical model quantifying drug release. *Eur. J. Pharm. Sci.* **15**: 355–366 (2002).
28. N. Faisant, J. Siepmann, P. Oury, V. Laffineur, E. Bruna, J. Haffner, and J. P. Benoit. The effect of gamma-irradiation on drug release from bioerodible microparticles: A quantitative treatment. *Int. J. Pharm.* **242**:281–284 (2002).
29. J. Crank. *The Mathematics of Diffusion*, 2nd ed., Clarendon Press, Oxford, 1975.
30. J. Wang, B. M. Wang, and S. P. Schwendeman. Characterization of the initial burst drug release from poly(D,L-lactide-co-glycolide) microspheres II: Alterations in surface permeability implicated in cessation of burst release. Proceedings AAPS Annual Meeting, Indianapolis, Indiana (2000).